Geophysical Research Letters

Supporting Information for

Determining bathymetry of shallow and ephemeral desert lakes using satellite imagery and altimetry

M. Armon[1], E. Dente[1,2,3], Y. Shmilovitz[1,2], A. Mushkin[2], T. J. Cohen[4], E. Morin[1], and Y. Enzel[1]

[1]The Fredy and Nadine Herrmann Institute of Earth Sciences, the Hebrew University of Jerusalem, Israel.

[2]The Geological Survey of Israel, Israel.

[3]Shamir Research Institute, University of Haifa, Israel.

[4]School of Earth and Environmental Sciences, University of Wollongong, Australia.

Contents of this file

Additional Supporting Information (Files uploaded separately)

Introduction

This supporting information file includes an explanation about the usage of water occurrence to divide Lake Eyre to sub-basins, and the neighborhood-weighting of pixel elevation values in it (text S1). This is followed by a description of the derivation of hypsometric curves (text S2) and of the usage of "wet" elevation measurements in Lago Coipasa (text S3). The figures at the end of this file (Figures S1-S14), and the attached movies (S1-S2) present additional features of the WOLP bathymetry methodology (elevation cross-sections, bathymetry maps not shown in the main text, etc.) and provide the specific ICESat-2 scan dates.

Text S1. Lake Eyre sub-basin division and neighborhood weighting of elevation values

1) Dividing Lake Eyre into sub-basins

Small variations in lake floor height in shallow and vast lakes are often manifested as several sub-basins. Such lakes show a complex relation of water occurrence and elevation (e.g., Figure 1c). To overcome this complexity, different sub-basins should be represented by different relations. We extracted sub-basins of Lake Eyre North using pseudo watersheds obtained from the water occurrence map (Figure 1a) in a similar manner to topographic analyses; routines of flow directions and fill were performed on the map of water occurrence residue from 100% using the TopoToolbox V2 (Schwanghart and Scherler, 2014). To use this approach, one must make sure the division into sub-basins meets two conditions (1) at least one (and preferably more) ICESat-2 scan overpassed the sub-basin, (2) the division into several drainage basins seems realistic (e.g., by comparison to satellite images; e.g., Movie S1). We found the division into five sub-basins in Lake Eyre North is an optimal balance between these two conditions (Figure S2). Specifically, we ensured at least four ICESat-2 scans in each sub-basin.

2) Neighborhood weighting of values in Lake Eyre

The relation between water occurrence and elevation in Lake Eyre (Section 3) was calculated separately for each of the sub-basins. Such calculation yields a step-like topography (Figure S13), at the boundaries of each basin. To avoid both this step, and the high sensitivity in elevation of each pixel to the exact sub-basin division, regions closer than ~11 km (400 pixels distance) to the pseudo water divide were assigned values from neighboring basins as well, inversely weighted according to their distance from the divide. The elevations near sub-basin boundaries were calculated using the following averaging, yielding the elevation of each pixel (h_i):

$$\begin{cases} d^*_{i,j} = 1 - \frac{d_{i,j}}{D}, & d_{i,j} < D \\ d^*_{i,j} = 0, & d_{i,j} \geq D \end{cases} \quad \text{(Eq. S1)}$$

$$w_i = \sum_{j=1}^{n} d^*_{i,j} \quad \text{(Eq. S2)}$$

$$h_i = \frac{1}{w_i} \sum_{j=1}^{n} h_{i,j} \cdot d^*_{i,j} \quad \text{(Eq. S3)}$$

where i is the pixel id, j is the sub-basin id, D is the maximum distance used for averaging, $d_{i,j}$ is the distance (number of pixels) between pixel i and the closest pixel in the j^{th} watershed, $h_{i,j}$ is the elevation calculated using the specific j^{th} sub-basin fit (as detailed in Section 2), n is the number of sub-basins, and w_i is the sum of weights ($d^*_{i,j}$) given to pixel i because of its proximity to watershed boundaries. Notice that if $d_{i,j} \geq D$ (i.e., when a pixel is farther from the watershed than the maximum distance for averaging) this calculation yields the same number as in a single watershed calculation ($h_{i,j}$). Namely, we consider this pixel as belonging to a single sub-basin.

Text S2. Calculations of the hypsometric curves and maximum lake depths

To calculate the hypsometric curves of the different lakes, a series of constant-value rasters were generated for each bathymetry (WOLP, SRTM, and LC12), with an elevation greater than the minimum elevation of the analyzed bathymetry. The increments of the constant-value rasters are 0.1 m. The bathymetries were kept in their original resolution (~30 m), without any

smoothing or sink filling. To calculate the area and volume of the lakes at different elevations, the ESRI ArcMap Cut-and-Fill tool was applied. Only the largest continuous area and the volume associated with it were extracted for each elevation. This methodology was chosen to simulate hydrologic connectivity during lake filling, and to clean out the filling of isolated regions within the bathymetry maps. Thus, the results of this procedure represent a filling stage of the lakes, rather than their desiccation stage.

In the northern and more frequently inundated area of Lago Coipasa, the "wet" bathymetric map features elevations that are lower than the "dry" WOLP map. These elevations were extrapolated, since no ICESat-2 scan passed through this region, and are therefore not identical. To have a common datum for the evaluation of the difference between the "wet" and the "dry" WOLP hypsometric curves of Lago Coipasa we shifted the height of the "wet" bathymetry by 0.7 m (negative values in Figure 3c). A similar procedure was applied to the SRTM map of Sabkhat El-Mellah, due to 10 m deep sinks in the original data.

Maximum lake depths were calculated based on WOLP bathymetry maps (and LC12 in Lake Eyre). The depths were derived from the difference between the minimum lake elevation and the elevation in which the area curves become asymptotic (i.e., the lake area reaches its maximum extent, based on data from Pekel et al., 2016) or the highest elevation of the bathymetric maps.

Text S3. Derivation of "wet" elevation scans in Lago Coipasa

Elevation measurements throughout this study are from the Advanced Topographic Laser Altimeter System (ATLAS) product #3 (ATL03) of the ICESat-2. Measurements used in the derivation of the bathymetry of Lago Coipasa were taken between October 2018 and May 2019 (Figure S8, S9). However, in February 2019 the lake was flooded (SM2).

The green light (532 nm) ATLAS measurements can give accurate water levels from the surface of a lake, however, they could also penetrate the water and give underwater floor elevation data in shallow environments (Parrish et al., 2019). A few methods to estimate which of the measurements are bottom readings exist. The basic idea is to derive the lowest data points that exhibit a continuous profile, which could either be done manually (Parrish et al., 2019), or using an algorithm accounting for the increased data point density at the lake bottom (Ma et al., 2019).

The difference in refraction coefficients between water and air yields an error in the horizontal geolocation of photon returns, which is minimized in nadiral photon returns (~9 cm for readings in water depth of 30 m; Parrish et al., 2019).

Parrish et al. (2019) provided an approximated equation to correct for the elevation difference in underwater photon returns:

$$Z' \approx Z + 0.25416D \qquad \text{(Eq. S4)}$$

where Z' is the corrected elevation, Z is the measured elevation, and D is the water depth, assuming a water refraction coefficient based on a temperature of 20°C and water salinity of 35 PSU (seawater). However, a freshwater salinity would yield roughly the same results (~0.5% difference).

To avoid horizontal offsets in this study, we use post-flood elevation data from only nadiral ATLAS profiles. Lake surface and water column data points were extracted manually, in places where the lake floor stands out (see an example for one scan profile in the figure below). To calculate the exact elevation, one needs to know the water depth, the angle between the laser beam and the water surface, and salinity and temperature of the water, most of which are hard to acquire in remote regions as Lago Coipasa. Because of the need for an optimization process

to find accurate water depths, and the relatively small bias expected when underwater corrections (Eq. S4) are applied, we did not correct this error. The expected bias due to a water depth of ~0.7 m, as in Lago Coipasa (see figure below) is <18 cm, which is still much lower than the SRTM data error (Table 1).

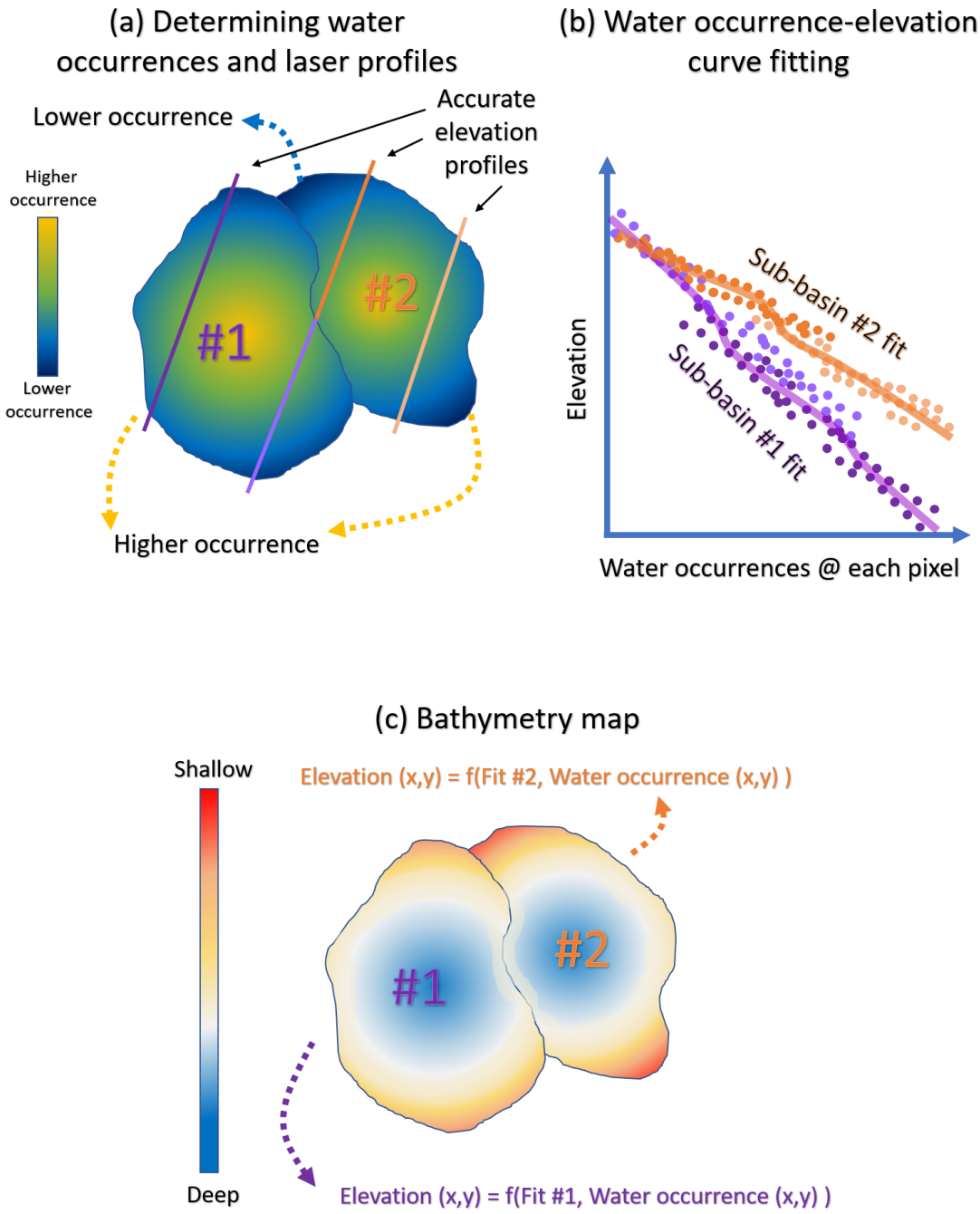

Figure S1. A schematic representation of the water occurrence-laser profiles (WOLP) method to derive bathymetries of shallow and ephemeral lakes. (a) Acquiring water occurrence from the global water occurrence map (Pekel et al., 2016) and ICESat-2 laser altimetry elevation data. Each laser profile is assigned to a specific sub-basin (marked in different colors). Pseudo sub-basins are identified using the water occurrence map. (b) Fitting occurrence-elevation curves for each of the sub-basins (#1 and #2) based on all laser altimetry profiles covering the specific sub-basin. (c) Application of the different fits for each sub-basin. The elevation at each pixel is determined by the fit of its assigned sub-basin, and by the water occurrence value at that pixel. Shallower bathymetry is inferred from low water occurrence values in individual

(~30 m) pixels during 1984-2015. Deeper bathymetry is inferred from high water occurrence. Please note the bathymetry is not directly related to the water-occurrence (compare the pattern of panels c and a), but rather to the obtained fits of each sub-basin.

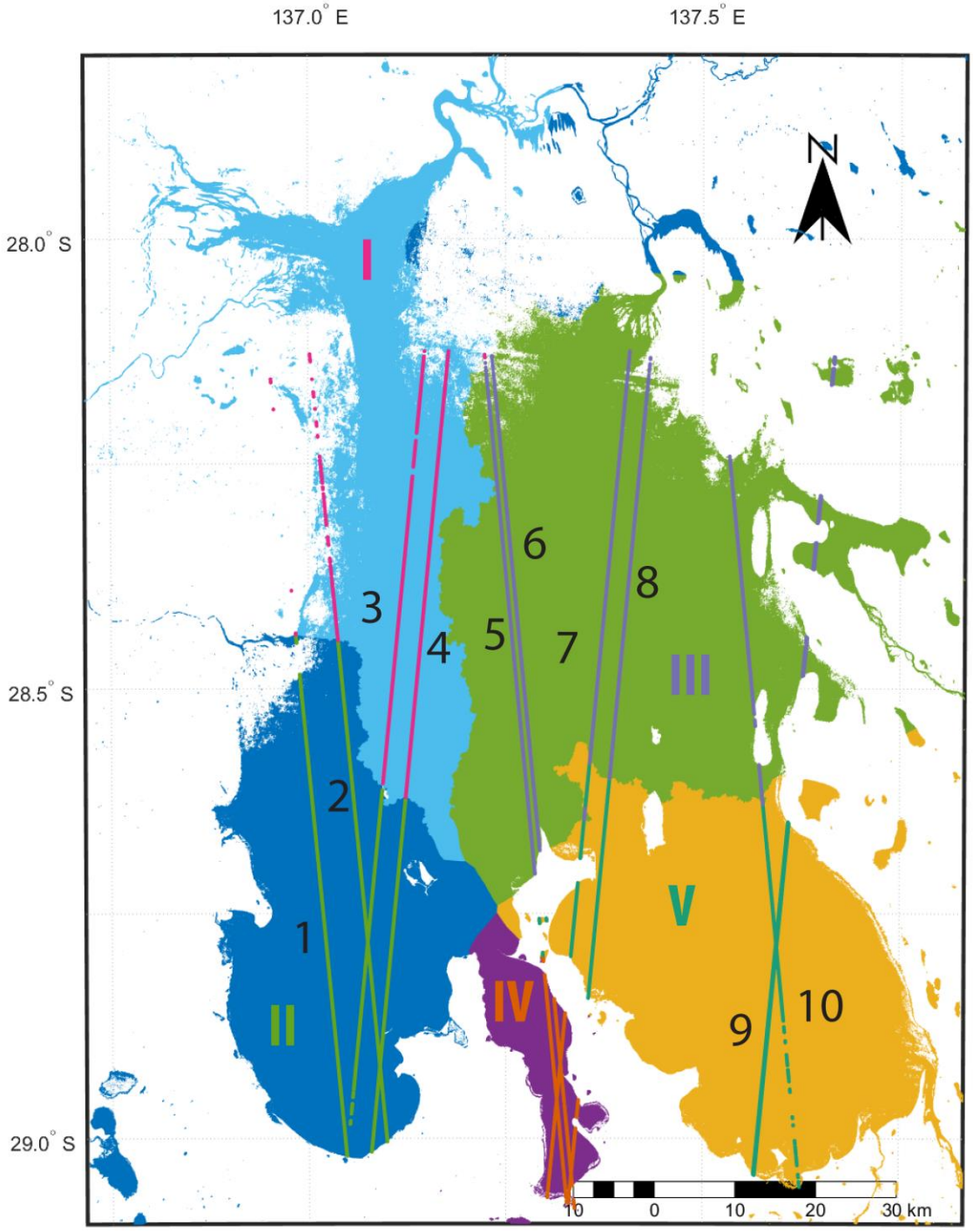

Figure S2. Sub-basins in Lake Eyre North (colored regions; labeled in Latin Numerals), and ICESat-2 scan profiles used in WOLP bathymetry derivation (labeled 1-10). Data from these scans were used according to their location in the various sub-basins. Scans 1-10 were taken during the following overpasses: 1 = 2019-03-06_t1046; 2 = 2018-12-06_t1046; 3 = 2018-11-20_t810; 4 = 2019-02-19_t810; 5 = 2019-04-04_t101; 6 = 2019-01-04_t101; 7 = 2018-12-

19_t1252; 8 = 2019-03-20_t1252; 9 = 2018-10-18_t307, 2019-04-18_t307; 10 = 2018-11-03_t543. Data were downloaded from: https://openaltimetry.org/data/icesat2/, from the ATL03 product: Neumann, T. A., A. Brenner, D. Hancock, J. Robbins, J. Saba, K. Harbeck, and A. Gibbons. 2019. ATLAS/ICESat-2 L2A Global Geolocated Photon Data, Version 1. Boulder, Colorado USA. NSIDC: National Snow and Ice Data Center. doi: https://doi.org/10.5067/ATLAS/ATL03.001. [last Accessed at 31/12/2019]. Note: only high confidence data points were used. WGS84 ellipsoid elevations were transformed into Australian Height Datum (Australian 2020 geoid) using Geoscience Australia website at: http://www.ga.gov.au/ausgeoid/.

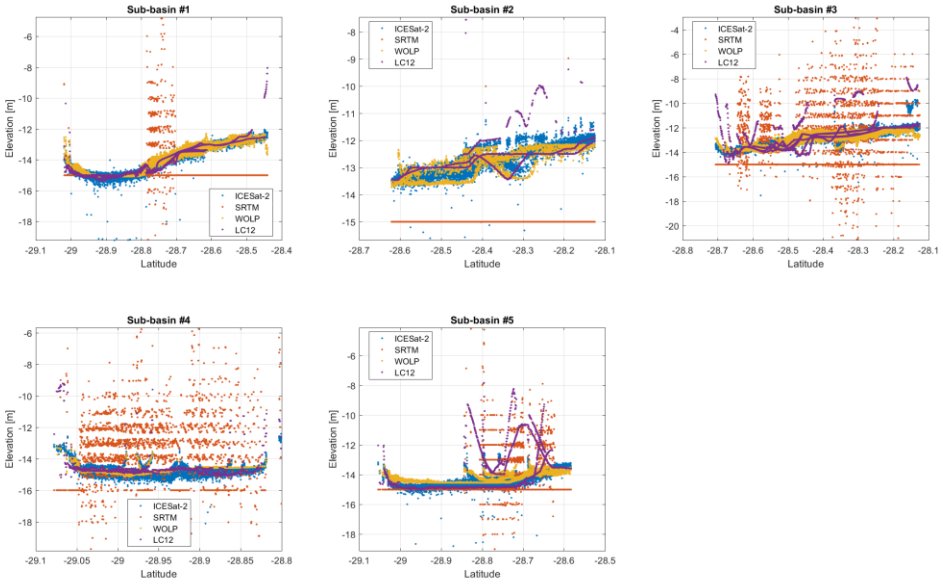

Figure S3. Elevations along ICESat-2 profiles at each of the sub-basins (Figure S2) of Lake Eyre from all data sources used in this study.

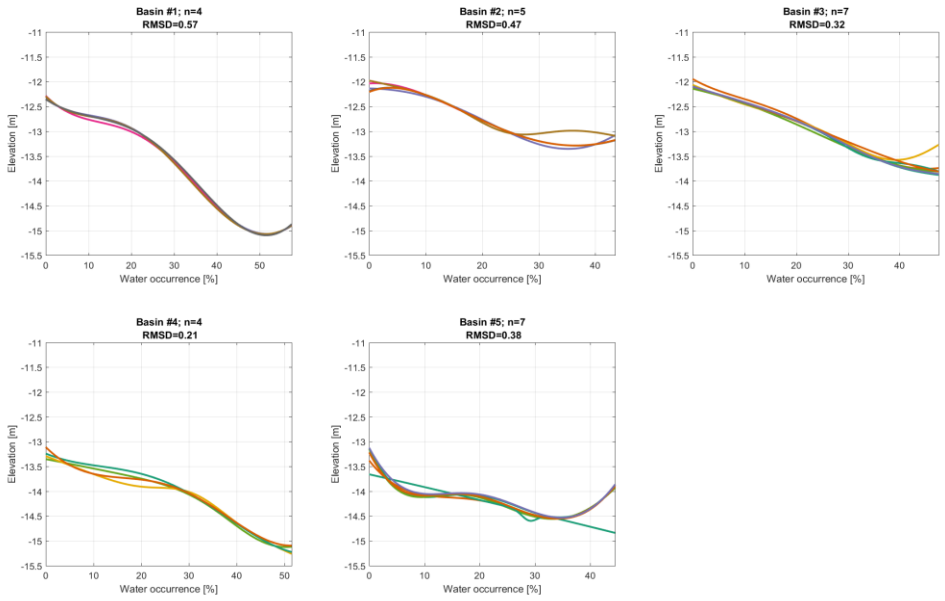

Figure S4. WOLP cross-validation results for each of the sub-basins (Figure S2) of Lake Eyre. Each curve is the 2-term Gaussian fit of ICESat-2 elevation data from all scans but one within a sub-basin, to water occurrence along scan profiles. The excluded scan was used to obtain RMSD values, and the average of these RMSD values is shown for each sub-basin. The number of scans for each sub-basin is denoted by "n".

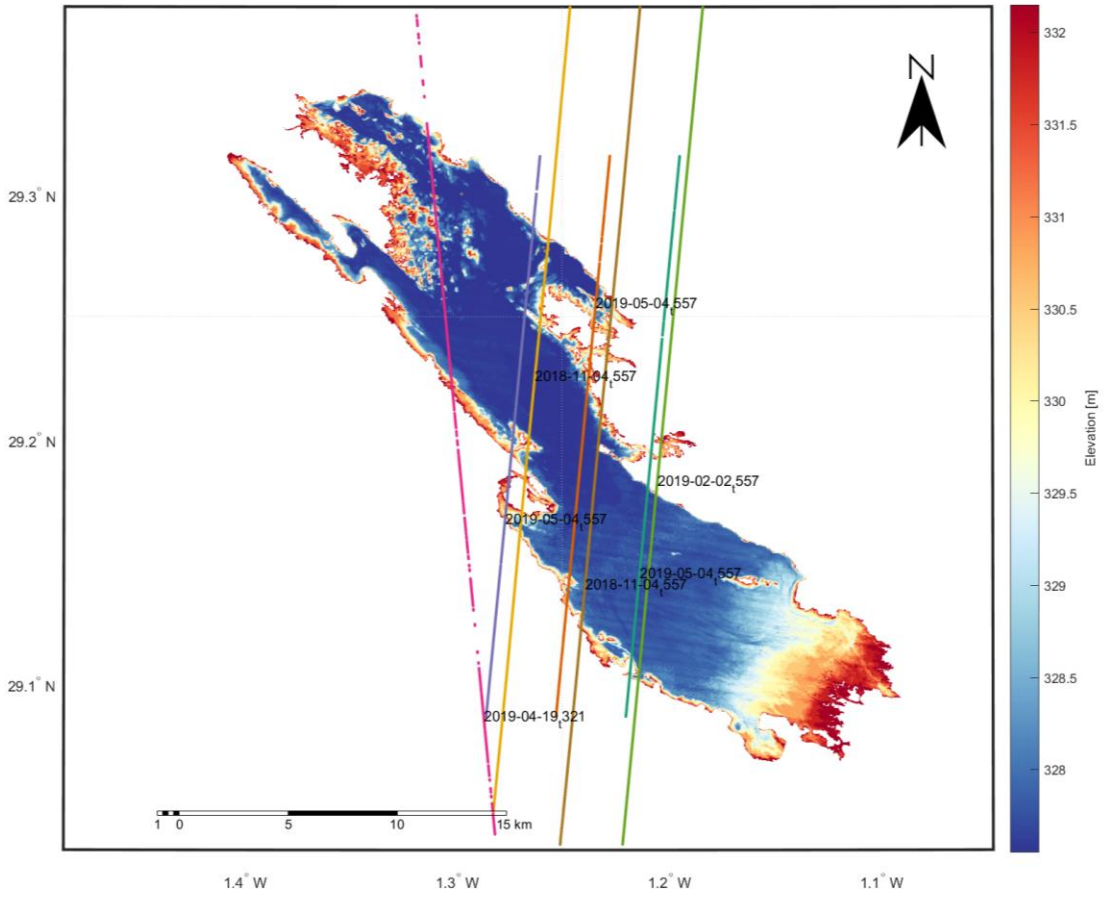

Figure S5. WOLP bathymetry of Sabkhat El-Mellah and ICESat-2 scans used to derive it. Scan dates and indices are listed next to each of the scans. Gray dots represent regions in which water occurrence is greater than the highest occurrence overpassed by ICESat-2.

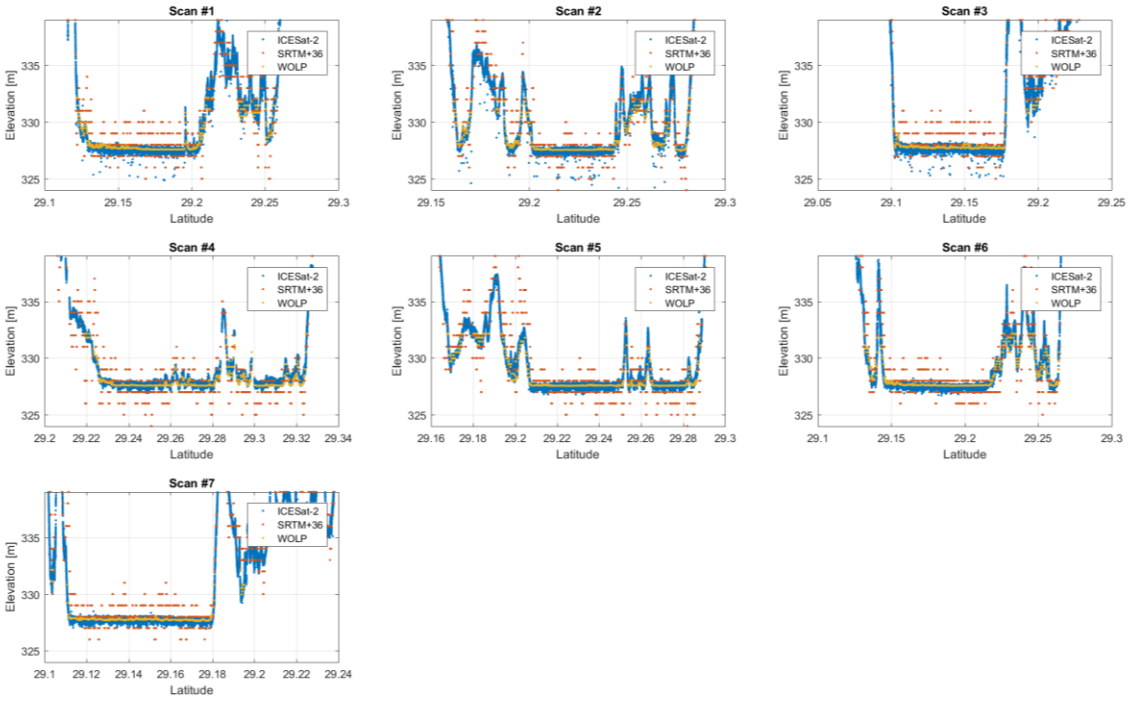

Figure S6. As in Figure S3, but for Sabkhat El-Mellah. SRTM elevation values were added a fixed correction value of 36 m, to compensate for the different vertical datum.

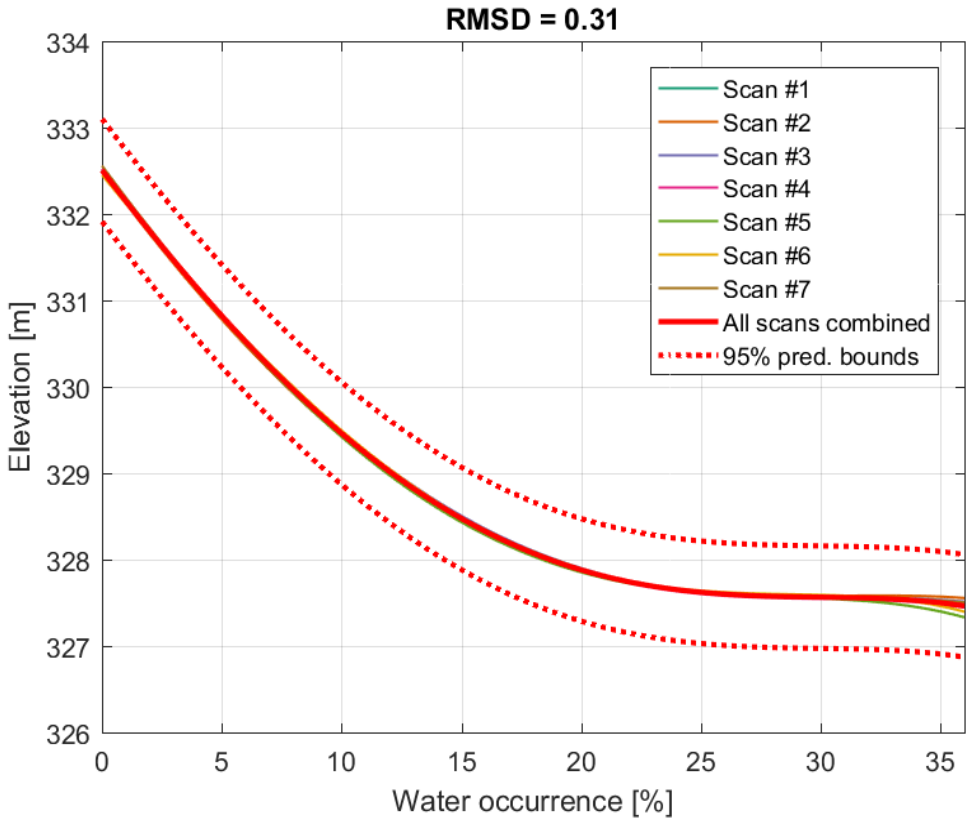

Figure S7. WOLP cross-validation results for Sabkhat El-Mellah. Each curve is the 2-term Gaussian fit of ICESat-2 elevation data from all scans but one, to water occurrence along scan profiles. The excluded scan was used to obtain RMSD values, and the average of these RMSD values is shown.

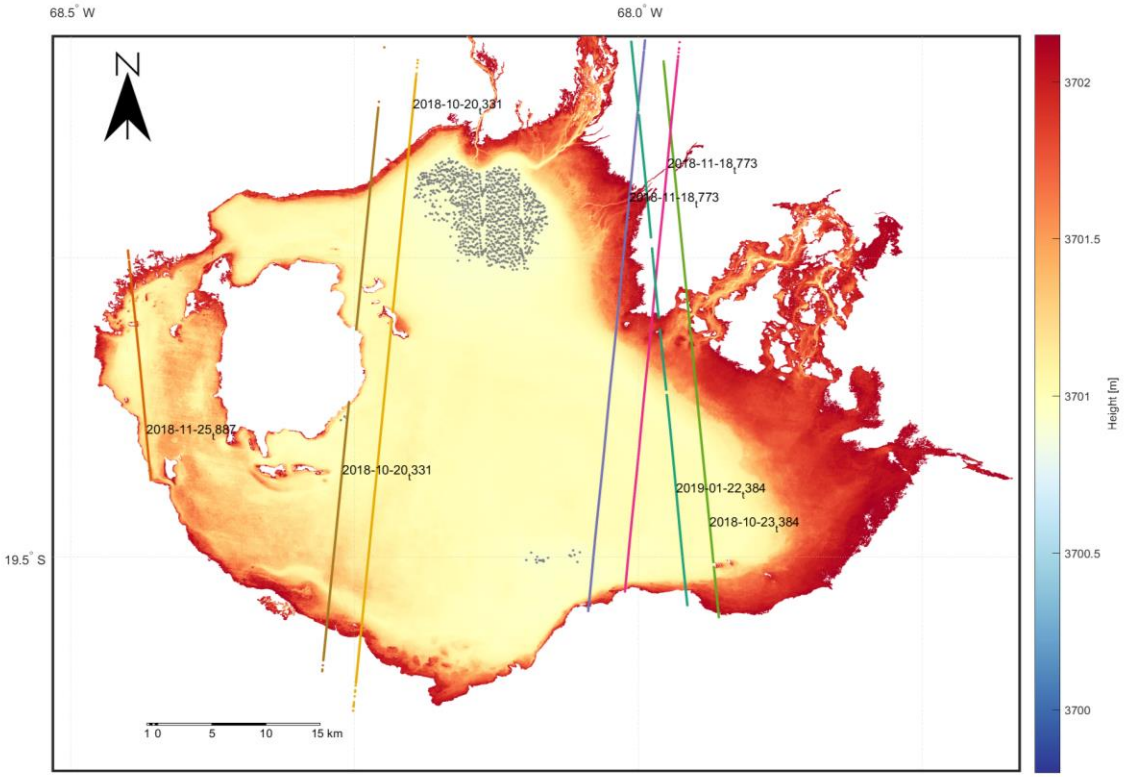

Figure S8. As in Figure S5, but for the "dry" WOLP bathymetry of Lago Coipasa.

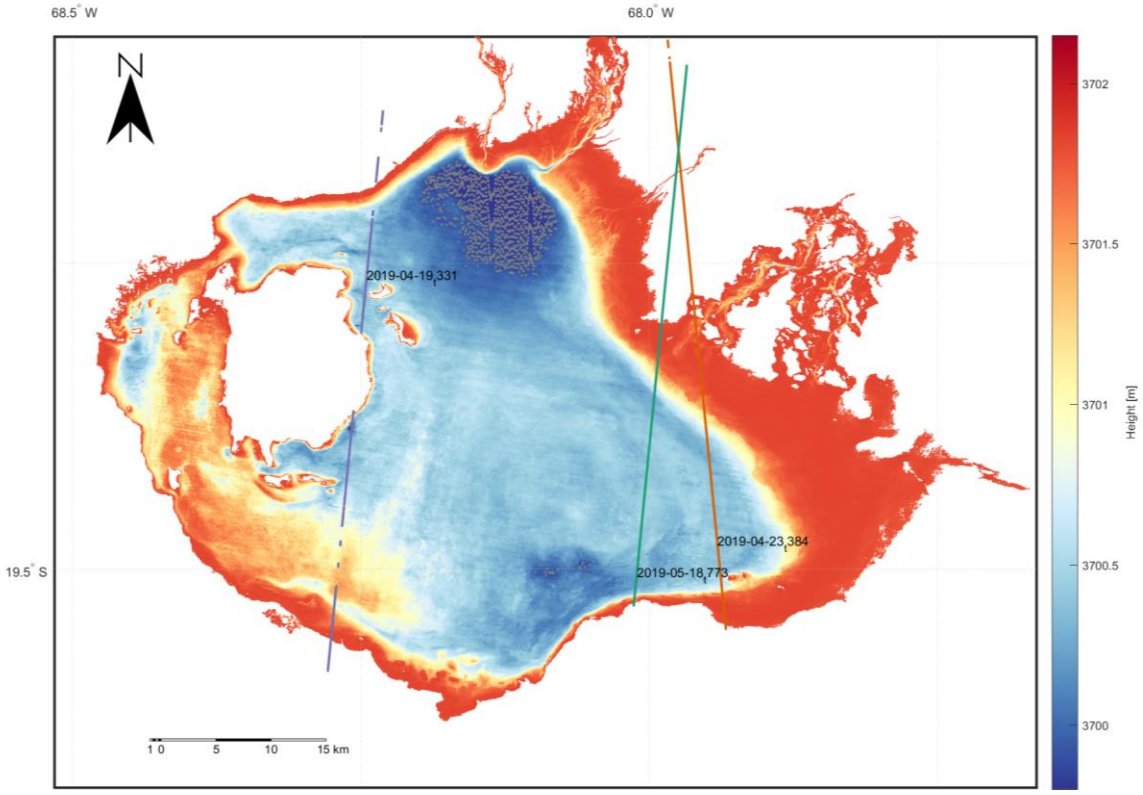

Figure S9. As in Figure S5, but for the "wet" WOLP bathymetry of Lago Coipasa.

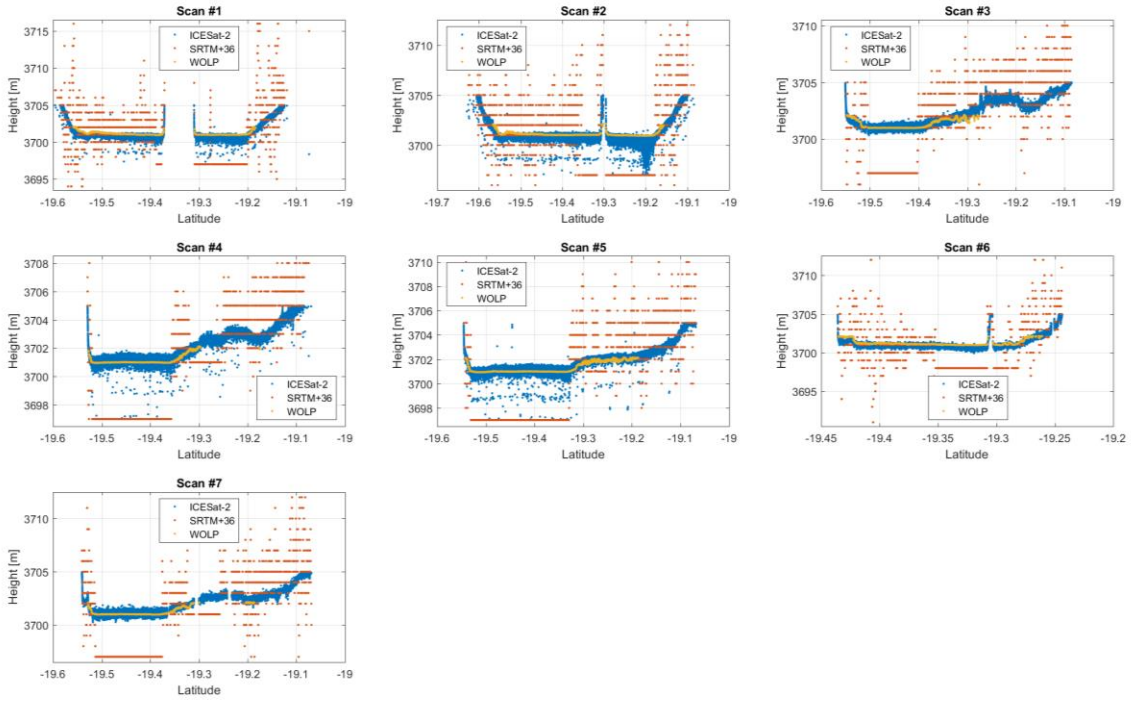

Figure S10. As in Figure S6, but for the "dry" WOLP bathymetry of Lago Coipasa.

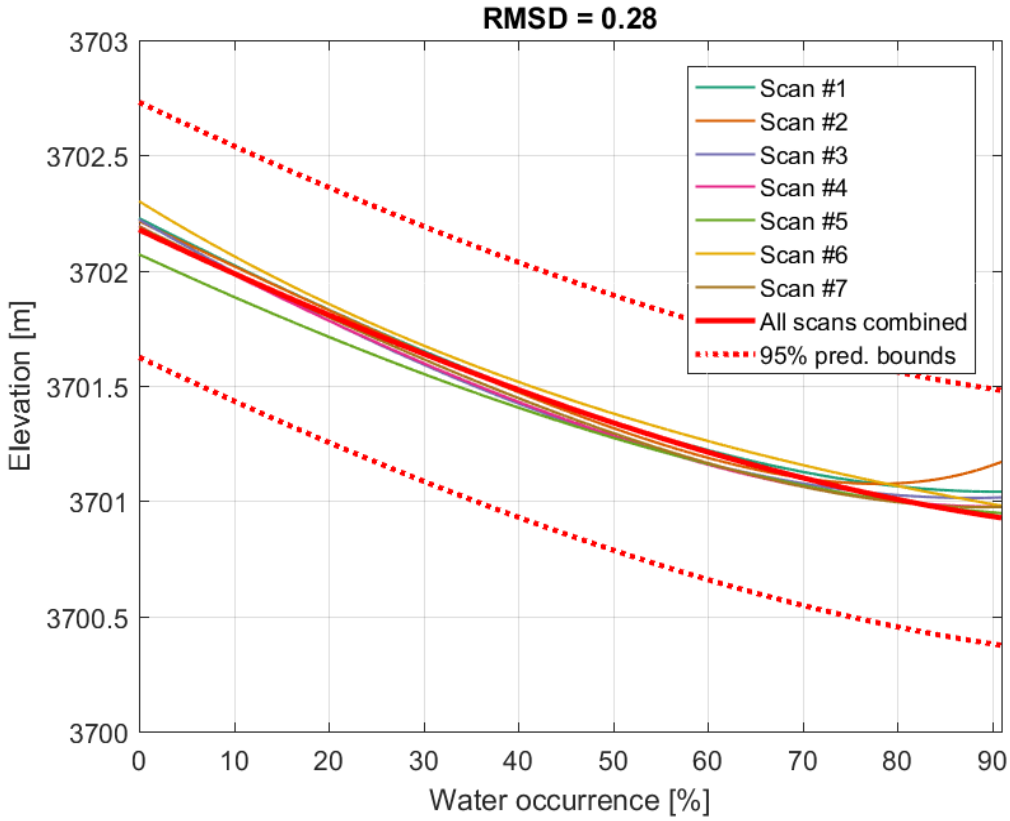

Figure S11. As in Figure S7, but for the "dry" WOLP bathymetry of Lago Coipasa. Fits were made using a 2-term exponential function.

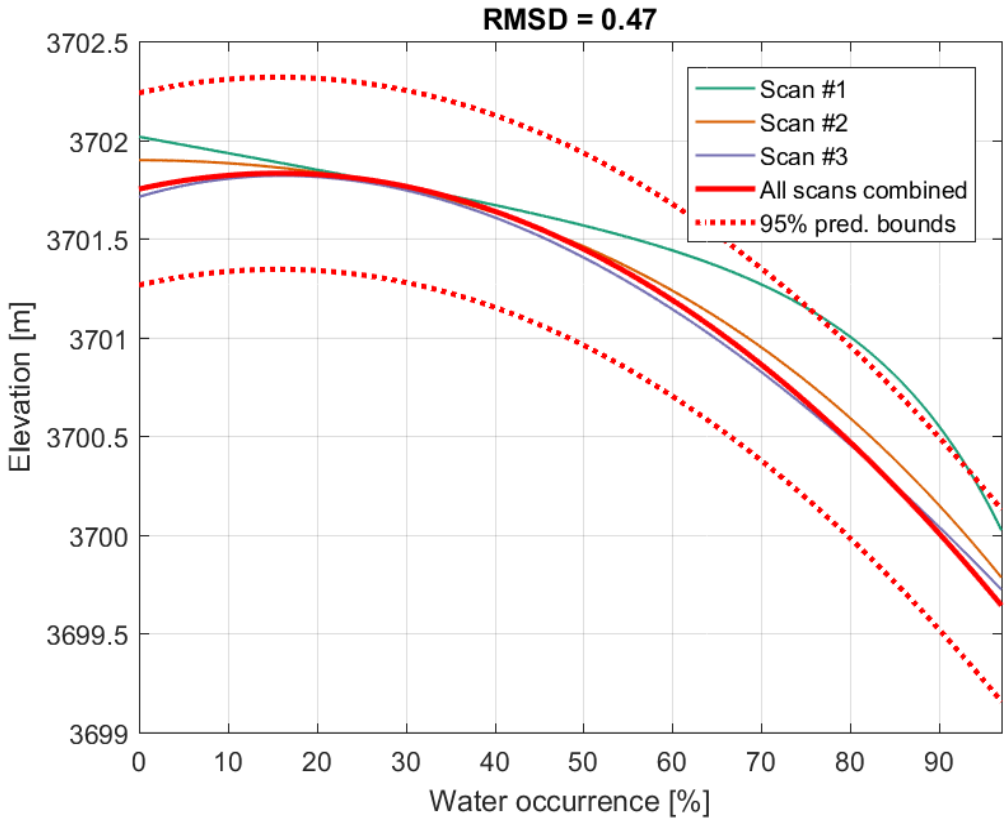

Figure S12. As in Figure S11, but for the "wet" WOLP bathymetry of Lago Coipasa.

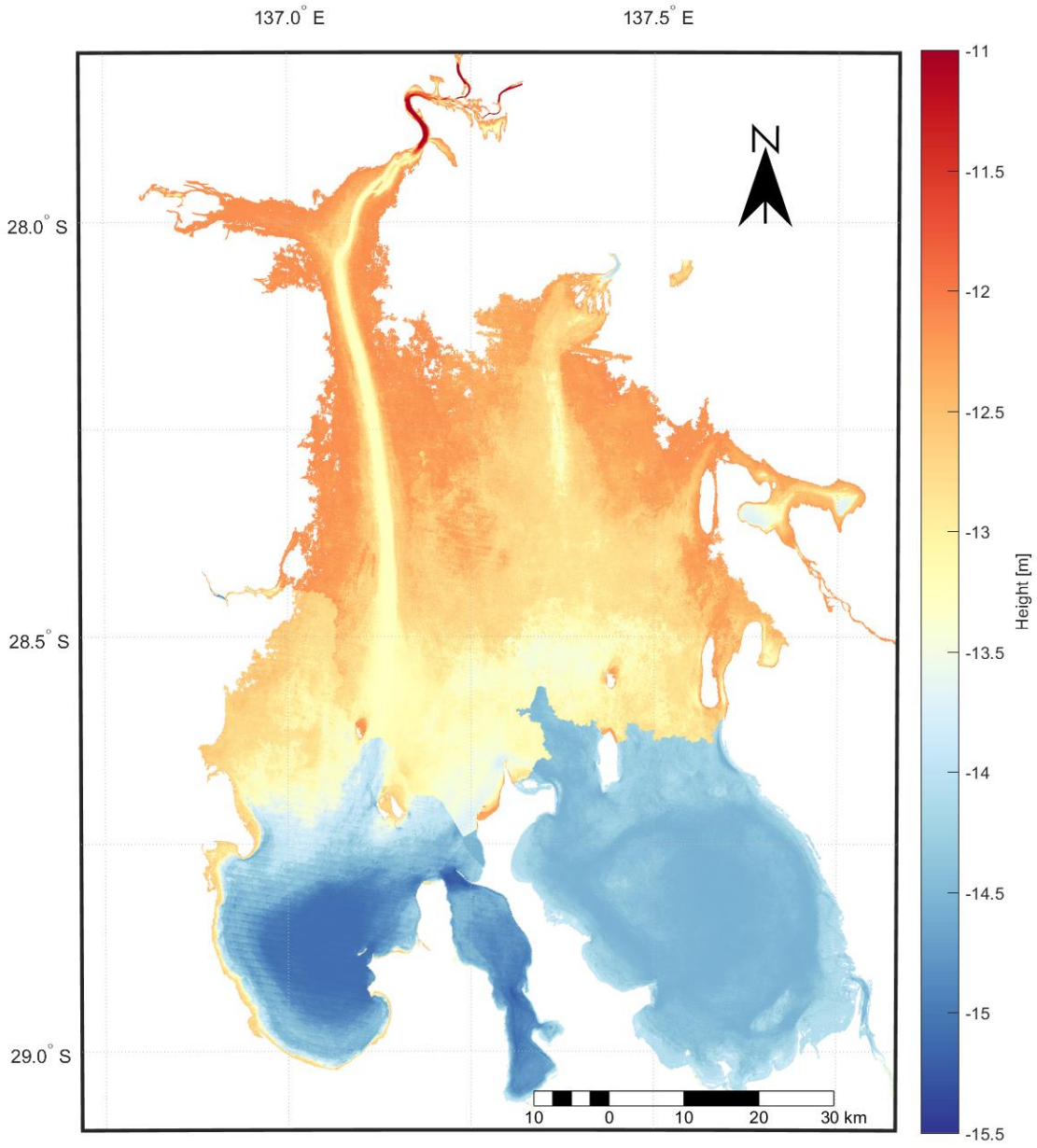

Figure S13. Step-like topography when ascribing each pixel with a single value based on the relation of water occurrence and elevation in each sub-basin. Please note the difference with respect to Figure 1d.

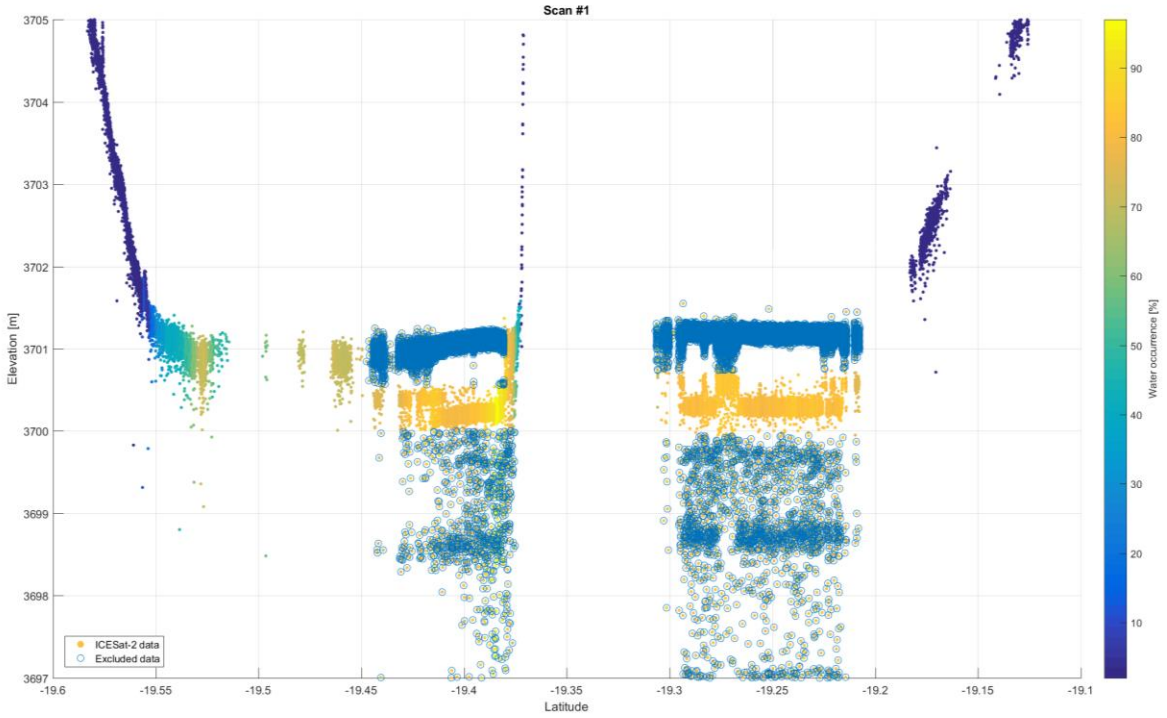

Figure S14. An example for lake-floor extraction in Lago Coipasa from "wet" scan #1 (Figure S9).

Movie S1. Time series of true-color satellite imagery of Lake Eyre showing floods that occurred between March and August 2019. Images are Copernicus Sentinel-2 data [2019], and were obtained from the Sentinel-hub website (https://apps.sentinel-hub.com/eo-browser/). Please notice the filling of the western sub-basin (Belt Bay), while the eastern sub-basin (Madigan Gulf) stays mostly dry throughout these floods.

Movie S2. Similar to Movie S1, but for the Lago Coipasa flood in February 2019.